Food and Energy Security

WILEY

Food and Energy Security Open Access

ORIGINAL ARTICLE OPEN ACCESS

Transcriptome Profiling of Resistance Gene Analogs in Soybean's Cross-Tolerance to Water Limitation and Rust Stress

Gustavo Husein[1] | Thiago Maia[2] | Fernanda R. Castro-Moretti[3] | Jessica D. K. Nunes[3] | Lilian Amorim[3] | Paulo Mazzafera[4] | Harm Nijveen[5] | Claudia B. Monteiro-Vitorello[1]

[1]"Luiz de Queiroz" College of Agriculture, Department of Genetics, University of São Paulo, Piracicaba, Brazil | [2]Department of Plant Pathology, Center for Plant Science Innovation, University of Nebraska-Lincoln, Lincoln, Nebraska, USA | [3]"Luiz de Queiroz" College of Agriculture, Department of Plant Pathology and Nematology, University of São Paulo, Piracicaba, Brazil | [4]Institute of Biology, Department of Plant Biology, University of Campinas, Campinas, Brazil | [5]Laboratory of Bioinformatics, Wageningen University, Wageningen, the Netherlands

Correspondence: Claudia B. Monteiro-Vitorello (cbmontei@usp.br)

Received: 9 September 2025 | **Revised:** 18 September 2025 | **Accepted:** 19 September 2025

Funding: This study was supported by the Fundação de Amparo à Pesquisa do Estado de São Paulo (FAPESP—2019/13191-5).

Keywords: abiotic stress | biotic stress | climate change | drought | *Phakopsora pachyrhizi*

ABSTRACT

Asian soybean rust (ASR), caused by *Phakopsora pachyrhizi*, is the most destructive foliar disease of soybean, with yield losses up to 90%. With climate change intensifying drought and expanding disease incidence, it is critical to understand how combined abiotic and biotic stresses influence plant defense. We investigated the transcriptomic response of a susceptible soybean cultivar to ASR infection under normal and water-limited conditions at four infection stages (12, 24, 72, and 192 h after inoculation). We observed a biphasic expression of defense-related genes, particularly resistance gene analogs (RGAs), with an early peak at 12 h and a late resurgence at 192 h. Combined stress induced a greater number of differentially expressed genes (DEGs) than rust alone, especially at early infection. Among the differentially expressed RGAs (RGADEs), over 64% belonged to the TM-LRR class, and NBS-LRR genes were the most enriched at known ASR resistance loci, particularly Rpp2. Water limitation strongly modulated gene expression at late stages, revealing stress-specific transcriptional reprogramming. These findings were consistent with the activation of potential cross-tolerance mechanisms in soybean, highlighted the temporal dynamics of RGADEs under dual stress, and provided potential targets for developing cultivars with improved resilience to both rust and water scarcity.

1 | Introduction

Soybean (*Glycine max* (L.) Merr.) is considered one of the most important crops globally due to its high protein and oil contents, making it a versatile nutritional resource for food, animal feed, and biofuel production (Rahman et al. 2023). The most destructive disease affecting soybeans and the source of severe epidemics is Asian soybean rust (ASR), caused by the fungus *Phakopsora pachyrhizi*. Without chemical control, soybean producers can face productivity losses between 20% and 90%, characterizing the ASR pathogen among the 12 most damaging plant pathogens globally based on its scientific and economic importance (Dean et al. 2012).

Projections of the incidence of *P. pachyrhizi*, considering both the selection pressure on soybeans and climatic changes, point to an increase in disease occurrence in cultivated areas (Alves et al. 2011; Ghini et al. 2007). Soil moisture stress, a significant factor in soybean production losses, is expected to worsen due to climate change (Leng and Hall 2019). Changes in historical

This is an open access article under the terms of the Creative Commons Attribution License, which permits use, distribution and reproduction in any medium, provided the original work is properly cited.

© 2025 The Author(s). *Food and Energy Security* published by John Wiley & Sons Ltd.

precipitation patterns will likely lead to more severe drought stress in key soybean-growing regions (Thornton et al. 2014). Climate change can further drive the expansion of pathogens and hosts, accelerating the spread of plant diseases to previously unaffected regions (Burdon and Zhan 2020; Delgado-Baquerizo et al. 2020). Moreover, it can indirectly influence plant-pathogen interactions by altering the biochemical, physiological, ecological, and evolutionary processes of both the host and the pathogen (Cheng et al. 2019; Trivedi et al. 2022; Velásquez et al. 2018). Consequently, the combined effects of biotic and abiotic stresses, such as reduced water availability and pathogen infection, on plant development are being studied more extensively (Camejo et al. 2005; Engelbrecht and Kursar 2003; Gerós et al. 2016; Mittler 2006; Palliotti et al. 2009). Additionally, understanding the genetic basis for resistance to these stresses and their interactions remains a critical area of interest (Kakumanu et al. 2012; Le et al. 2012; Xue et al. 2013).

The presence of ASR drastically reduces the photosynthetic capacity of the contaminated leaves. It causes severe defoliation of the plants, effectively reducing the number of pods per plant and the quality and number of seeds (Echeveste Da Rosa 2015). Fungicides are regularly used to control the fungus. However, in addition to the potentially harmful effects on the environment and the fungicide's high costs, the low sensitivity of *P. pachyrhizi* to some active ingredients is reducing the availability of effective chemical compounds. Thus, to control ASR, there is a need for more efficient and lasting forms of control (Godoy et al. 2016; Ivancovich et al. 2007; Langenbach et al. 2016).

Among these alternatives, superior soybean varieties with high productivity and resistance to ASR appear to be the most effective way to control the disease (Vuong et al. 2016). To date, soybean cultivars resistant to ASR have been mapped mainly to seven loci, named Rpp 1 to 7, which are specific genomic regions associated with varying degrees of resistance to *P. pachyrhizi* (Childs et al. 2018; Goellner et al. 2010; Kelly et al. 2015; King et al. 2016; Pedley et al. 2019). The loci Rpp1 (Hyten et al. 2007), Rpp4 (Silva et al. 2008), and Rpp6 (Li et al. 2012) are all located on chromosome 18 but at different positions. Additionally, other Rpp loci are found on distinct chromosomes: Rpp2 (Silva et al. 2008) on chromosome 16, Rpp3 (Hyten et al. 2009) on chromosome 6, Rpp5 (Garcia et al. 2008) on chromosome 3, and Rpp7 (Childs et al. 2018) on chromosome 19.

From a functional perspective, immunity has been organized into two layers depending on the cellular response, either by activating extracellular receptors (TM-LRR), also known as pattern recognition receptors (PRR), and usually related to pattern-triggered immunity (PTI), or activating intracellular receptors (NBS-LRR), encoded by disease resistance (R) genes and related to effector-triggered immunity (ETI) (Dodds et al. 2024). These receptors with potential plant resistance activity are collectively termed resistance gene analogs (RGAs) (Sekhwal et al. 2015). Independent of the RGA class, after apoplastic or intracellular perception, the immune response converges to a similar set of downstream events that will potentially prevent infection. These include processes such as reactive oxygen species (ROS) production, calcium influx, signaling transduction by mitogen-activated protein kinases (MAPK), defense gene expression, and defense hormone production (DeFalco and Zipfel 2021).

Next-generation sequencing (NGS) technologies opened opportunities to identify genome-wide, based on sequence similarity, RGAs that encode proteins with structural similarities to *R* genes and their transcription profile when pathogens challenge plants (Rody et al. 2019; Sekhwal et al. 2015). Notably, RGAs often form clusters in plant genomes, which may include functionally related genes that are not necessarily similar in sequence (Chang et al. 2002). This clustering, driven by ancient whole-genome duplications and segmental duplications followed by gene deletions and genomic reorganizations, has expanded RGA families (Michelmore and Meyers 1998; Perazzolli et al. 2014). Identifying these potential resistance-associated genes and mapping their genomic organization is highly beneficial for plant breeding. This information supports the development of selection strategies that facilitate the early selection of resistant cultivars, reducing costs through approaches such as marker-assisted selection (MAS) (AliFakheri 2014; Echeveste Da Rosa 2015).

In a previous report (Castro-Moretti et al. 2024), we observed that water limitation enhanced disease severity caused by *P. pachyrhizi* in soybean, significantly changing the leaf metabolic profile. Complementing this previous report, our study aimed to reveal the comparative expression pattern of a susceptible genotype under the influence of reduced water availability in the severity of ASR. Furthermore, we identified RGAs that were differentially expressed across infection stages under these conditions. Our results provide a better understanding of key mechanisms involved in disease progression for targeted strategies to develop ASR-resistant soybean cultivars addressing yield stability and global food security.

2 | Materials and Methods

2.1 | Experimental Design, Plant Material and Inoculation

As an obligatory phytopathogen, the *P. pachyrhizi* inoculum was maintained in a greenhouse by regularly inoculating soybean plants. To achieve this, 8 to 10 soybean seeds were sown weekly until they reached the V4 stage. These plants were watered daily until the soil was fully saturated and inoculated with a rust spore solution (10^5 urediniospores.ml^{-1}) in a humid chamber at 23°C in the dark for 24 h.

The experiment was developed using a fully randomized factorial design, with three biological replicates per treatment of the susceptible soybean commercial cultivar BMX Lança IPRO. These treatments included plants with and without the presence of biotic and abiotic stresses independently, and leaf samples collected at four time points, resulting in the generation of 16 treatments. Soybean plants were kept under two water availability levels: a moderate water deficit, defined as 65% of the plant-available soil water capacity, and a control group of plants cultivated with 80% soil water capacity. The humidity estimation of the soil mixture, prepared in a

2:2:1 (v/v/v) ratio of soil, sand, and manure, at the permanent wilting point was conducted using the procedure detailed by Ferreira (2010). To verify the water status of the treatments, three fresh V2 trifoliate leaves were collected just prior to the inoculation (performed at 7:00 p.m.), and analyzed for relative water content, following the method described by Barrs and Weatherley (1962).

The plants were grown under controlled temperature conditions in a greenhouse until the development stage V4 for the experimental treatments with controlled water availability. Water control for these plants began 48 h before inoculation, ensuring that the treatments were well established. The plants were weighted daily and watered according to their respective water capacity—80% (control treatment) or 65% (water limited). The plants were then inoculated with the fungus suspension at the same maintenance concentration at 7:00 p.m. Inoculated and mock plants were covered with plastic bags and incubated in the dark in a humid chamber at 23°C (±2°C) for 24 h. Fungal inoculated and mock plants were maintained separately to avoid cross-contamination of the control plants. After this incubation period, the plants were returned to the greenhouse, where the controlled water conditions were maintained throughout the experiment. One V3 trifoliolate leaf per plant was collected at times 12, 24, 72, and 192 h after inoculation (HAI) and immediately frozen with liquid nitrogen and stored at −80°C until the extraction of total RNA.

2.2 | Total RNA Extraction and Sequencing

Total RNA extraction was performed sequentially: first using the Trizol method (Sigma-Aldrich, St. Louis-MO, USA), followed by RNA purification with the Purelink RNA mini kit (Invitrogen, Carlsbad-CA, USA), according to the manufacturer's instructions. After extraction, total RNA was treated with DNAse 1 (Sigma-Aldrich, St. Louis-MO, USA), and RNA quality was verified with electrophoresis on a 1.5% agarose gel and further observation under UV light (2100 Bioanalyzer, Agilent Technologies, Santa Clara, USA). Quantification and purity were verified in a NanoDrop 2000 UV Visible Spectrophotometer (Thermo Scientific, USA).

The RNA library construction by poly-A enrichment was performed using the Illumina TruSeq Stranded mRNA kit (Illumina Inc., USA), followed by paired-end sequencing using an Illumina NextSeq 2000 with read lengths of 100 bp and an average of 10 million clusters or 20 million paired-end reads per sample. In total, 48 independent libraries were sequenced, corresponding to four collection times, two fungal conditions (with and without the presence of the fungus), two water availability regimes (with and without water limitation), and three replicates.

2.3 | Data Processing

The quality of the reads generated in the sequencing was verified through the software SeqKit (version 0.16.1) (Shen et al. 2016). After quality verification, reads were mapped against the Soybean reference genome *Glycine max* (Schmutz et al. 2010) version 4 using the program HISAT2 (version 2.1.0) (Kim et al. 2015). Then, the aligned reads were assembled in their possible transcripts and the gene abundance was estimated using StringTie (version 2.2.1) (Pertea et al. 2015). Subsequently, the prepDE script provided by StringTie was used to generate a count matrix, with genes represented in rows and samples in columns. For each time point, genes with a read count exceeding 10 in at least one sample were retained, a mild and commonly applied prefiltering step that minimizes the influence of low-abundance transcripts and reduces random noise in downstream analyses. Expression levels of the remaining genes were normalized using the DESeq2 method (Love et al. 2014).

2.4 | Gene Expression and Functional Annotation

Principal Component Analysis (PCA) was conducted to explore gene expression patterns using data that was normalized and variance-stabilized transformed (VST) for all genes with the statistical R package DESeq2 (Love et al. 2014). This approach allowed for examining the overall variation in the dataset and visualizing the separation of samples based on the influences of time, biotic stress, and abiotic stress on gene expression. The identification of differentially expressed genes (DEGs) was also performed using DESeq2, considering genes with a False Discovery Rate (FDR) < 0.05 as differentially expressed.

The over-representation analysis (ORA) of the Gene Ontology (GO) biological process terms enriched in the DEGs was performed using the package topGO (Alexa and Rahnenfuhrer 2024) from the Bioconductor project (BiocManager v3.18) implementing the Kolmogorov–Smirnov test and the "classic" algorithm. This approach was selected because it incorporates gene ranking based on expression changes, allowing the detection of subtle, coordinated transcriptional responses not captured by binary enrichment methods such as Fisher's exact test.

2.5 | Resistance Gene Analogs (RGAs)

The RGAs (resistance gene analogs) were analyzed using the encoded proteome of the Soybean reference genome for all different possible gene's isoforms, based on the characteristics conserved among the resistance genes (*R*) (Hammond-Kosack and Jones 1997). To this end, six different tools were used to predict resistance gene domains and motifs: (1) Coils v2 (Lupas et al. 1991); (2) TMHMM v2 (Krogh et al. 2001); (3) InterProScan v5.33–72.0 (Zdobnov and Apweiler 2001); (4) PfamScan with Pfam v32.0 (Bateman et al. 2004); (5) Phobius (Käll et al. 2004); and (6) TargetP 2.0 (Almagro Armenteros et al. 2019).

Each predictor can identify conserved features among the *R* genes by structural analysis. Following the classification framework proposed by Rody et al. (2019), only sequences containing at least one of the three conserved domains of the RGAs—LRR, NB-ARC, or NB-LRR—were kept to form the set of candidate RGAs for the

Soybean reference genome. These candidates were then mapped to their chromosomal locations and grouped into clusters using the same criteria: clusters consisted of at least three putative RGAs of any class if there were no more than nine other genes between two RGAs or if the distance between them was less than 250 kb.

While RGA classification was performed at the isoform level due to the potential variability in domain architecture introduced by alternative splicing, downstream expression analyses were conducted at the gene level. In this case, the first annotated isoform for each RGA gene was used as a representative to summarize expression values, including for heatmap visualization.

3 | Results

3.1 | Transcriptome Data Analysis

A total of 48 RNA-Seq libraries were generated from leaf tissues of *Glycine max* cv. BMX Lança IPRO, sampled under eight combinations of biotic (Asian soybean rust) and abiotic (water limitation) stress treatments, each applied with and without the respective stress factor, across four time points (12, 24, 72, and 192 h after inoculation), with three biological replicates per condition. High-quality sequencing reads were obtained from all libraries (Table S1). Subsequent quality control and mapping against the *Glycine max* Wm82.a4.v1 reference genome resulted in an average overall read alignment rate of 93.6%. This process identified 86,256 transcripts associated with 52,872 unique genes. After filtering out low-expression genes, 40,012 genes remained, encoding 75.7% of the predicted soybean proteome.

3.2 | Differential Gene Expression Profiling

Visualization of the first two components of a Principal Component Analysis (PCA) of the samples revealed a predominant clustering effect attributed to the time factor (Figure 1). These two components explained 87% of the total variance. Given the predominant clustering by time points, we focused on the specific impact of the other two factors on gene expression. For each time point and per water limitation condition, we compared samples treated with the pathogen against those without the pathogen, resulting in eight pairwise comparisons.

As a result of this analysis, 9680, 3229, 932, and 1004 differentially expressed genes (DEGs) were obtained for plants in normal water conditions at times 12, 24, 72, and 192 h after inoculation (HAI), respectively. For water-limited plants, the numbers were 12,666, 1554, 1170, and 4352 DEGs at the same time points (Figure 2, Table S2). Notably, the most significant number of DEGs occurred at 12 HAI in both water regimes, accounting for nearly 65% of all DEGs detected. This peak suggests that 12 HAI represents a critical window for transcriptional reprogramming related to pathogen perception and the early activation of defense responses. Additionally, the number of DEGs at 12 HAI was approximately 33% higher in water-limited plants, indicating that water deficit may intensify or accelerate the plant's early response to infection.

We also analyzed the overlap between DEGs from different time points and treatments (Figure 2) with the objective of identifying shared stress-response genes that may contribute to cross-tolerance mechanisms. The highest number of total DEGs and

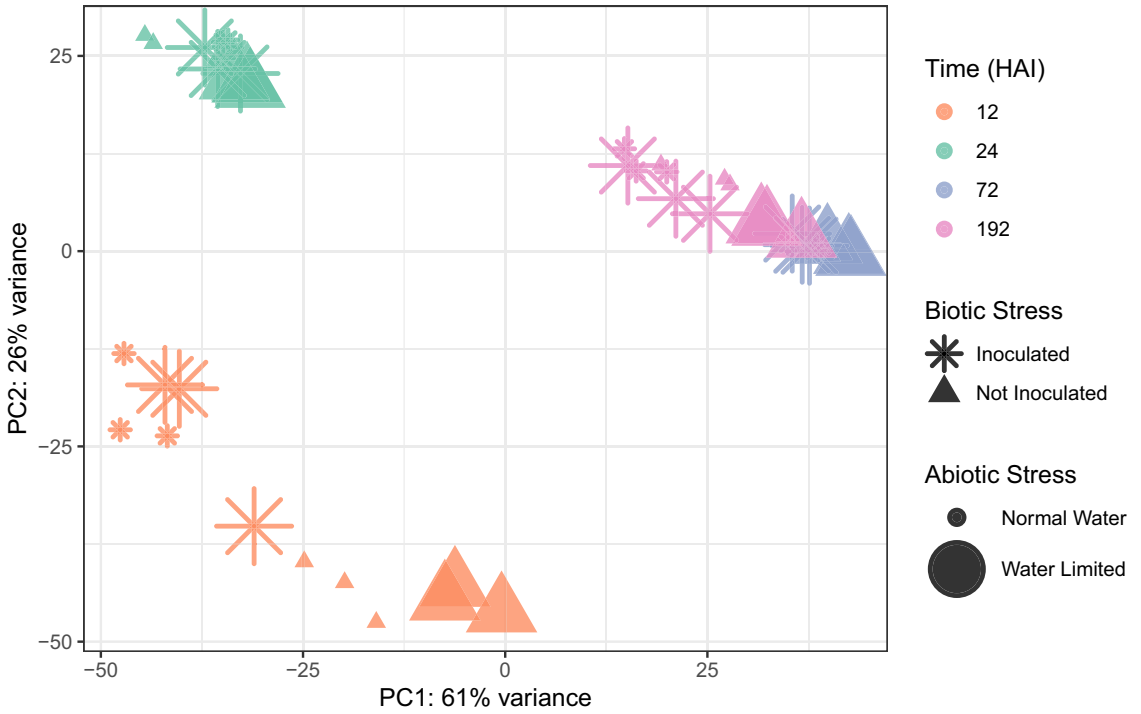

FIGURE 1 | First two components of a Principal component analysis (PCA) of gene expression profiles across time points (12, 24, 72, and 192 HAI) and experimental conditions. Each point represents a biological replicate, colored according to the time point, shaped according to the inoculation treatment (asterisks for inoculated and triangles for non-inoculated samples), and sized according to water availability (smaller symbols for normal water conditions and larger symbols for water-limited conditions).

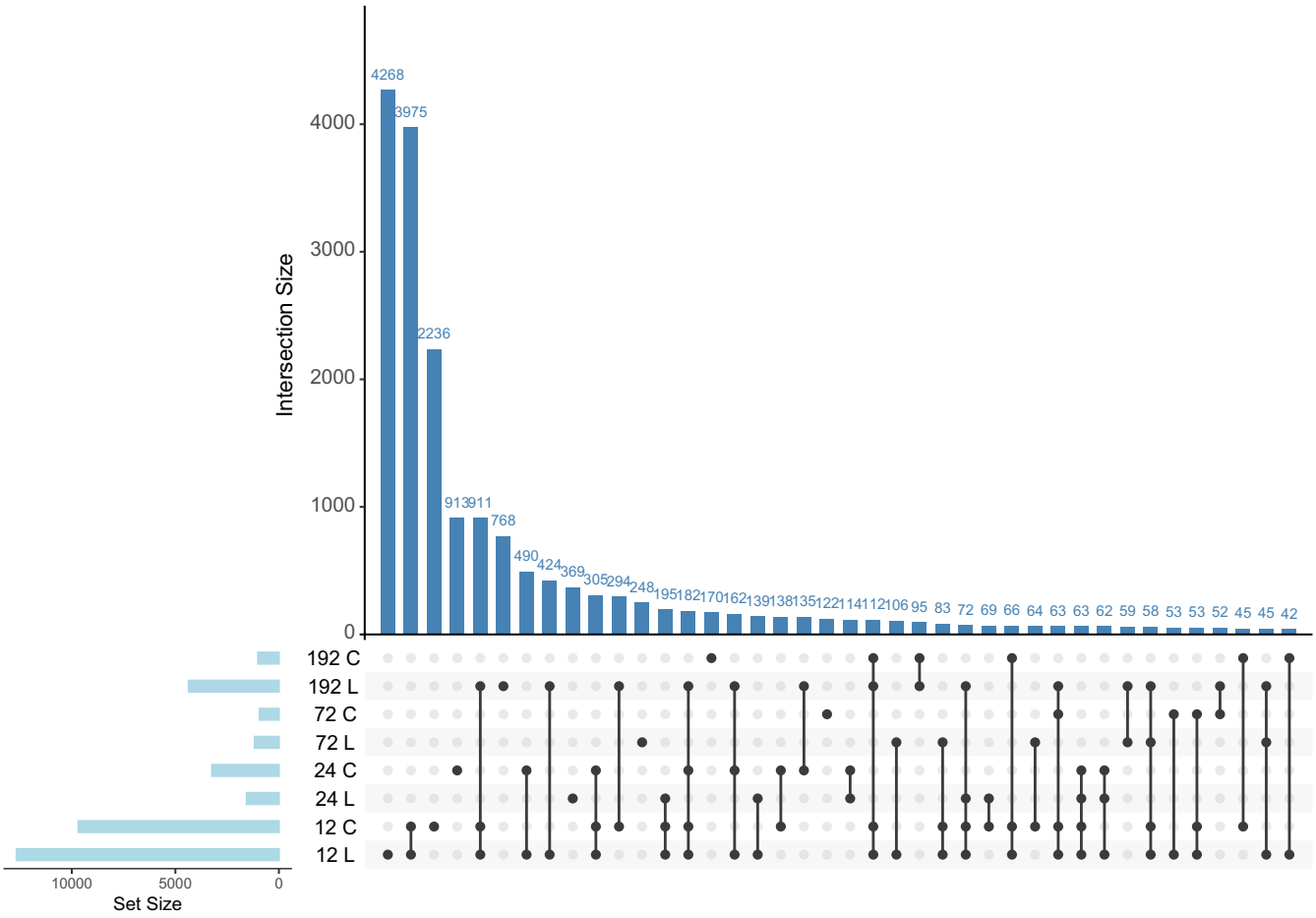

FIGURE 2 | Intersection and number of DEGs across all time points (12, 24, 72 and 192 HAI) and water condition (L: Water-limited/C: Control). DEGs were identified by comparing pathogen-inoculated samples against non-inoculated samples within each condition and time point, resulting in eight pairwise comparisons. The horizontal bars on the left represent the total number of DEGs identified per condition, while the vertical bars indicate the size of DEG intersections between different conditions. Black dots connected by lines specify the comparisons contributing to each intersection. The numbers above the bars represent the exact intersection sizes.

shared DEGs was observed at the earliest time point (12 HAI), indicating extensive transcriptional changes at this stage across conditions.

3.3 | Gene Ontology (GO) Enrichment Analysis of DEGs

To identify functional categories potentially enriched in DEGs, we conducted an overrepresentation analysis (ORA) to detect Gene Ontology (GO) terms associated with biological processes in which genes statistically showed differential expression greater than expected by chance. GO enrichment analysis (Table S3, Figures S1 and S2) of DEGs across all time points identified a cumulative total of 2503 significant GO terms in control plants and 2351 in water-limited plants. At 12 HAI, terms related to photosynthesis were prominently enriched in both conditions. In addition, control plants showed specific enrichment for response to oxidative stress. At 24 HAI, water-limited plants displayed enriched terms associated with phenylpropanoid biosynthesis, response to stimulus, and defense response. In contrast, control plants showed a broader spectrum of enriched GO terms at this time point, including response to stress, defense response, response to chitin, and response to hypoxia. These differences reflect condition-specific transcriptional reprogramming in response to infection. At 72 HAI, water-limited plants displayed enrichment for protein phosphorylation, signaling, response to stress, and defense response, whereas control plants showed enrichment for defense response and response to fungus. Finally, at 192 HAI, water-limited plants highlighted processes such as response to stress, defense response, response to biotic and abiotic stimulus, and photosynthesis, while control plants enriched GO terms primarily associated with photosynthesis.

3.4 | Plant Defense-Related GO Terms

Next, for the plant defense-related GO terms, we calculated the median $\log_2$ fold change (LFC) of the DEGs (Inoculated vs. Non-Inoculated) per GO term, which represents a quantification of the variation between the expression of genes in plants with the presence of the pathogen compared to plants without the presence of the pathogen. These values were used to demonstrate the variation that the presence of abiotic stress caused in the average expression of genes grouped into

biological processes associated with the plant defense response (Figure 3). The statistical significance of the differences between the expression levels of control and water-stressed plants is provided in Table S4.

At the beginning of the infection process (12 HAI), upregulated genes were associated with response to oxidative stress, phenylpropanoid biosynthetic process, and flavonoid biosynthetic process, with more pronounced expression changes under water-limited conditions. Concurrently, defense response and response to biotic stimulus were exclusively observed under these conditions. By 24 HAI, the expression levels of these defense-related genes were significantly decreased. In plants under water limitation, defense gene expression returned to basal levels, whereas in control plants, the genes were negatively regulated, showing expression levels below the basal threshold. At 72 HAI, there was a renewed increase in the expression of defense-related genes, particularly notable in plants not subjected to water stress, including genes specifically associated with fungal response, which were positively regulated. This upward trend persisted and intensified until 192 HAI, when defense gene expression remained elevated, especially in plants without water limitation.

3.5 | Water Deprivation Effect

To identify the effect of water deprivation on gene expression during infection, DEGs were analyzed between water-limited and control plants, both inoculated with the pathogen. The top 10 most enriched GO terms for each time point are shown in Figure 4. At the beginning of the infection process (12 HAI), enrichment is primarily focused on processes related to general metabolic pathways, such as the phenylpropanoid biosynthetic process and secondary metabolite biosynthetic process, alongside stress-related categories such as response to oxidative stress. By 24 HAI, broader stress responses dominate, including terms such as response to organic substance and response to abiotic stimulus. At 72 HAI, terms associated with defense response and response to chemical stimulus remain enriched, reflecting a continuation of general stress responses. However, at 192 HAI, following an extended period of water limitation, a notable shift occurs, with the emergence of genes specifically associated with water-related stress responses, such as response to water deprivation.

3.6 | Prediction of Resistance Gene Analogs (RGAs)

Using domain prediction tools and a custom Python3 script, the predicted Soybean proteome was scanned for candidate RGA identification, which was subsequently classified based on their combinations of predicted domains (see Material and methods). A total of 4076 gene isoforms were predicted to encode RGAs classified according to their domain configuration (Figure 5A; Table 1). Clustering of the predicted RGAs showed that these genes are distributed throughout the genome, with an accumulation of RGAs toward the chromosome ends (Figure 5A).

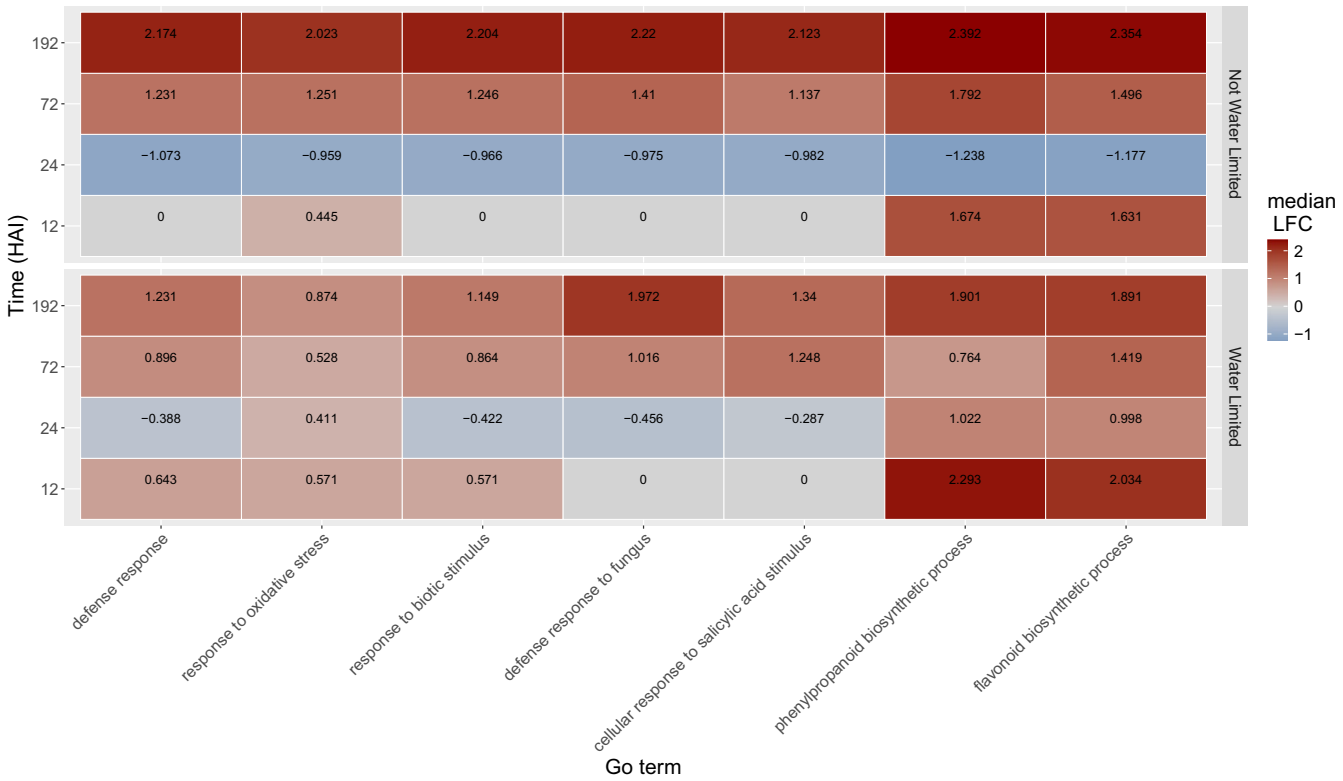

FIGURE 3 | Median $\log_2$ fold change (LFC) of genes annotated with GO terms related to plant defense response. Non-water-limited plants are represented at the upper part of the graph and the water-limited ones at the bottom. Each row represents a time of collection, while each column represents a GO term associated with plant defense response.

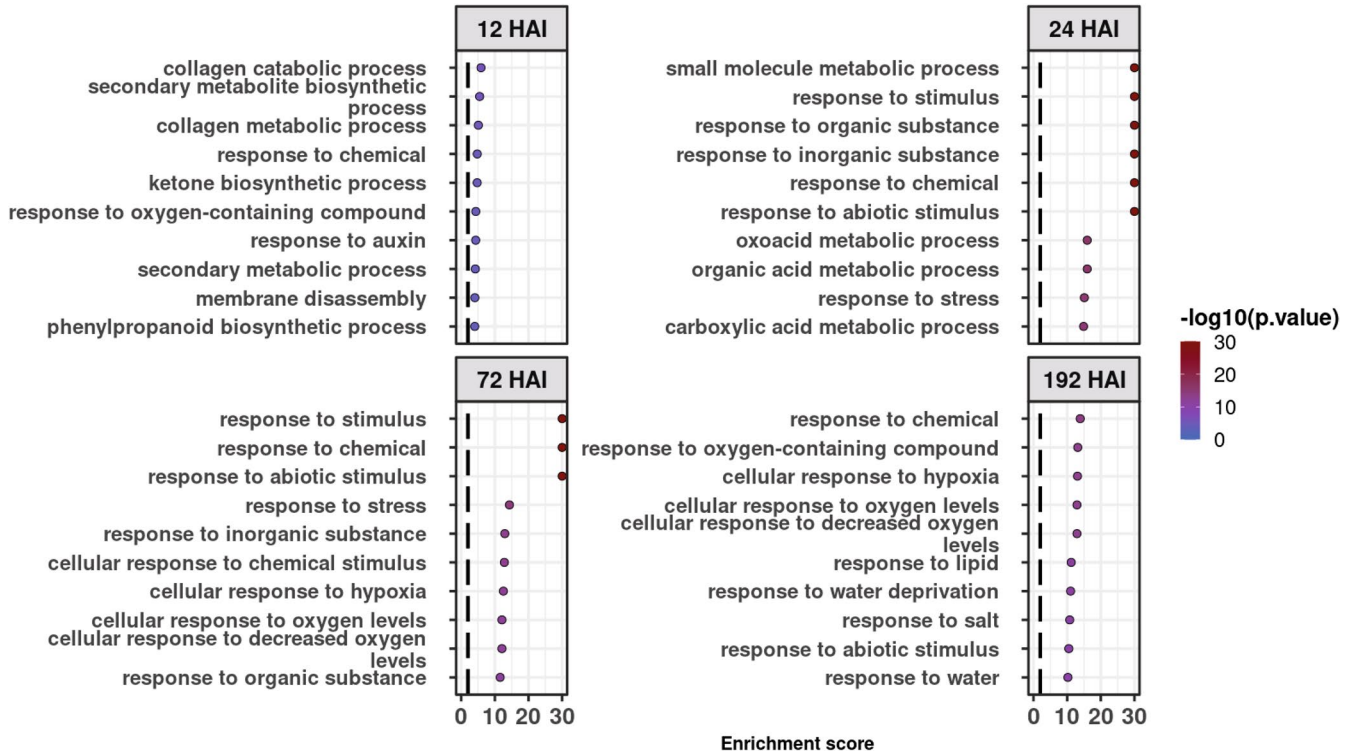

FIGURE 4 | Top 10 enriched Gene Ontology (GO) terms across time points (12, 24, 72, and 192 HAI) for DEGs identified from the comparison between water-limited and control plants inoculated with the pathogen. GO enrichment analysis was performed to identify biological processes (BP) significantly associated with DEGs at each time point. The x-axis represents the enrichment score, while the y-axis lists the enriched GO terms. The color gradient represents the statistical significance ($-\log_{10}$ (p-value)), with darker shades indicating higher enrichment significance. The vertical dashed line corresponds to a p-value threshold of 0.01.

Five classes of RGAs were predicted most frequently: CNL: coiled coil (CC) associated with NB-ARC and leucine-rich repeats (LRR); TNL: TIR domain associated with NB-ARC and LRR; RLK: receptor-like kinase; RLP: receptor-like protein; and TM-CC: transmembrane domain associated with a coiled-coil domain (Table 1). Differentially expressed RGA (RGADE) isoforms were detected on all chromosomes; however, chromosomes 2, 6, 8, 13, 16, and 18 harbored the highest numbers, together representing nearly 50% of all identified RGADEs (Figure 5B; Table 1). The most frequently predicted RGA classes were those containing a transmembrane domain, including RLK and RLP (TM-LRR encoding class), as well as the TM-CC subclass. Considering the total number of RGAs predicted in the genome, they correspond to 53%, and among DEGs, they represent 64% of all expressed RGAs combining both water conditions. This tendency further intensified when DEGs were separated based on water limitation, reaching 68% for plants under normal water conditions. On the other hand, in conditions with only biotic stress, the proportion of these RGAs aligned more closely with the overall set of RGADEs, maintaining around 64%.

When assessing the effect of water limitation, we observed notable variations in RGADE expression between plants exposed to water limitation and those maintained under controlled conditions, when compared to the reference genome. For instance, the TNL subclass exhibited expression exclusively under water limitation; isoforms from the RLK subclass were expressed in both conditions but at a higher level in control plants, and the RLP subclass showed a more moderate expression profile.

The presence of the pathogen affected the proportion of RGAs relative to the total number of gene isoforms. In the reference genome, 4076 out of 66,210 gene isoforms (6.15%) were classified as RGAs. This proportion was higher among DEGs obtained by comparing inoculated versus non-inoculated plants, with 1827 out of 19,165 DEGs isoforms (9.53%) identified as RGAs. Under water-limited conditions, 1451 out of 15,452 isoforms (9.39%) were classified as RGAs, compared to 1184 out of 12,653 isoforms (9.36%) under control conditions. These results demonstrated an enrichment of RGAs among DEGs driven by pathogen inoculation, with no substantial impact from water stress on the proportion of RGAs among expressed genes.

The timing of RGADE expression largely coincides with early pathogen invasion, particularly at 12 HAI, when tissue penetration is critical. Under water limitation, 1074 (56.76%) of RGADEs were expressed at 12 HAI, followed by a sharp drop to 112 (5.91%) at 24 HAI, 136 (7.18%) at 72 HAI, and 570 (30.12%) at 192 HAI. In contrast, under non-limiting water conditions, 788 (55.85%) of RGADEs were expressed at 12 HAI, 313 (22.18%) at 24 HAI, 203 (14.38%) at 72 HAI, and only 107 (7.58%) at 192 HAI (Figure S3; Table S5). These results suggest that water availability modulates the temporal distribution of RGADE expression, particularly at later infection stages, although further studies are needed to confirm the underlying mechanisms.

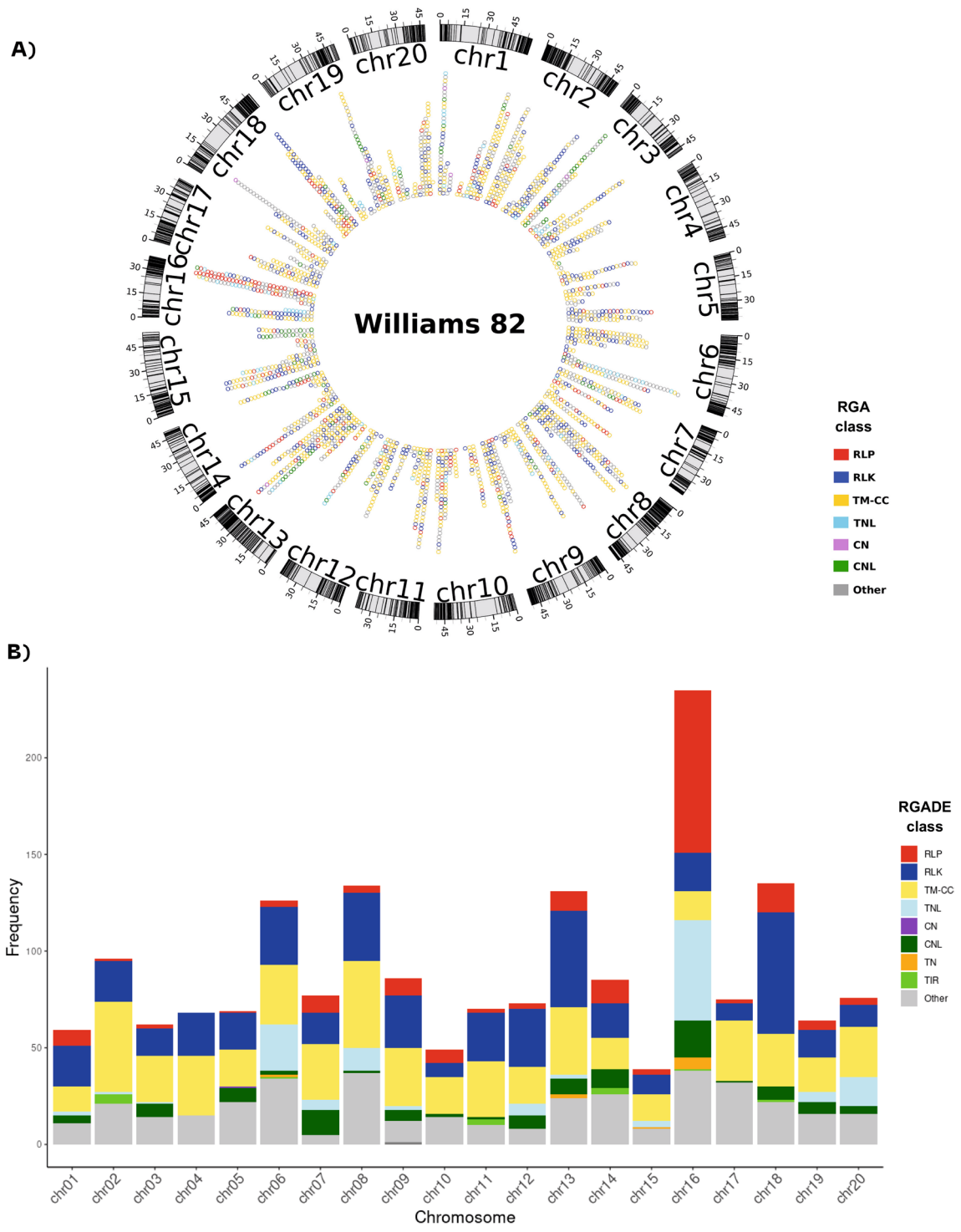

FIGURE 5 | (A) Distribution of the predicted RGAs in the Glycine max genome, mapped across the 20 chromosomes. The predicted RGAs are classified into subclasses, which are represented by different colors. The outer ring indicates chromosome locations in millions of base pairs. (B) Chromosomal distribution of differentially expressed RGAs (RGADEs) isoforms grouped into subclasses based on their predicted functional domains. The bar heights represent the frequency of each subclass per chromosome, and the colors correspond to the RGA subclasses in (A).

3.7 | Expression Profile of Resistance Gene Analogs Differentially Expressed

After exploring RGA isoform-specific expression, we collectively examined the expression profiles of the 932 RGADEs at the gene level (Figure S4). We observed a distinct temporal expression pattern between plants exposed to limited water and control plants. Under water-limited conditions, 54.85% of RGADEs were identified at 12 HAI, followed by 6.77% at 24 HAI, 8.48% at 72 HAI, and 29.9% at 192 HAI. In contrast, control plants exhibited a markedly different distribution, with 50.71% of RGADEs expressed at 12 HAI, 24.15% at 24 HAI, 15.96% at 72 HAI, and only

TABLE 1 | Number of putative RGAs by domain family and their classes in the reference genome and DEGs (up and down regulated combined).

RGA class	Whole genome	Overall DEGs	Water limited DEGs	Control DEGs
NBS-LRR encoding				
CNL	264 (6.48%)	106 (5.80%)	58 (4.00%)	86 (7.26%)
TNL	225 (5.52%)	130 (7.11%)	115 (7.92%)	43 (3.63%)
TN	26 (0.64%)	10 (0.55%)	10 (0.69%)	7 (0.59%)
CN	9 (0.22%)	3 (0.16%)	3 (0.20%)	3 (0.25%)
TM-LRR encoding				
RLK	916 (22.47%)	464 (25.40%)	372 (25.64%)	345 (29.14%)
RLP	340 (8.34%)	189 (10.35%)	149 (10.27%)	126 (10.64%)
Other variants				
TM-CC	1158 (22.41%)	518 (28.35%)	416 (28.67%)	337 (28.46%)
TL	1 (0.02%)	1 (0.05%)	0 (0%)	1 (0.08%)
TIR	50 (1.23%)	14 (0.76%)	14 (0.96%)	8 (0.68%)
Other	1087 (26.67%)	392 (21.45%)	314 (21.64%)	228 (19.25%)
Total number of RGAs	4076 (100%)	1827 (100%)	1451 (100%)	1184 (100%)

9.18% at 192 HAI. These results highlighted a pronounced enrichment of RGADE expression at 192 HAI under water-limited conditions, while control plants showed a more uniform distribution of RGADEs across earlier time points, particularly at 24 and 72 HAI.

Of the RGAs identified within the Rpp loci (55 genes), 28 were differentially expressed (RGADEs). These RGADEs were distributed across most loci and treatments, except for Rpp7 (Figure 6). At 12 HAI, the water limitation resulted in the induction of RGADEs of classes TNLs (6), RLK (1), and Other (3), whereas control plants downregulated RGADEs of classes TM-CC (1) and TNLs (4). At 24 HAI, RGADEs were nearly absent in water-limited plants, while control plants displayed a diverse expression pattern, including both upregulated (e.g., 2 Other and 5 TNLs) and downregulated (e.g., 3 Other, 1 TN, and 1 CNL) RGADEs. At 72 HAI, both conditions resulted in upregulated genes in low numbers. By 192 HAI, plants exposed to water stress showed exclusively upregulated RGADEs of most classes: TNLs (4), RLP (1), Other (3), TM-CC (1), and TN (1), while control plants had only one upregulated TM-CC.

The highest numbers of differentially expressed RGAs were found at the Rpp2 (12 RGADEs, 43%) and Rpp3 (10 RGADEs, 35.7%) loci, followed by Rpp1 (4 RGADEs, 14.3%) and Rpp5 (2 RGADEs, 7.1%) (Figure 6). Across all loci and treatments, the TIR-NBS-LRR (TNL) class was the most represented, accounting for 52% of the differentially expressed RGAs.

4 | Discussion

The interaction between climate-induced changes in global water availability and the susceptibility for plant diseases such as Asian Soybean Rust (ASR) remains unpredictable and critically important for the future of crop breeding (Jorge et al. 2015; Konapala et al. 2020). For some time, various authors have been exploring the crosstalk between biotic and abiotic stresses, considering their effect as either positive or negative in different pathosystems (Choudhary and Senthil-Kumar 2024; Singh et al. 2023; Sunarti et al. 2022). Also, we cannot assume that individual responses to different stresses can predict the effects of combined stresses (Pandey et al. 2015). As already demonstrated in diverse pathosystems (Paoletti et al. 2001; Ragazzi et al. 1995; van Niekerk et al. 2011), water deficit imposes a significant drought-stress penalty on plants, which has been widely associated with the aggravation of fungal diseases (Swett 2020) and negative impacts on crop development (Ghosh and Roychoudhury 2024). The effects of drought facilitate pathogen colonization, increase disease incidence, and exacerbate symptom severity due to the suppression of the plant defense mechanisms (Boyer 1995; Swett 2020). These findings support the notion that water availability may influence the effectiveness of plant defenses against fungal pathogens.

In this context, we examined the impact of water limitation on the transcriptomic response of a susceptible soybean genotype to *P. pachyrhizi*, analyzing infected leaves at four specific time points. The time points chosen represent key phases of the fungal infection process, including the formation of appressoria, cuticle penetration, and the invasion and subsequent growth of hyphae within the host tissue, observed at 12, 24, 72, and 192 h post-infection, respectively (Gupta et al. 2023).

The first overall analysis revealed that time had the most profound effect on the transcriptome, irrespective of the inoculation state. The pairwise comparison per time point of inoculated plants vs. inoculated plants under limited water conditions showed that genes related to plant defense (GO:0006952) had an intensified response in plants under water limitation at the early stages of infection. This effect

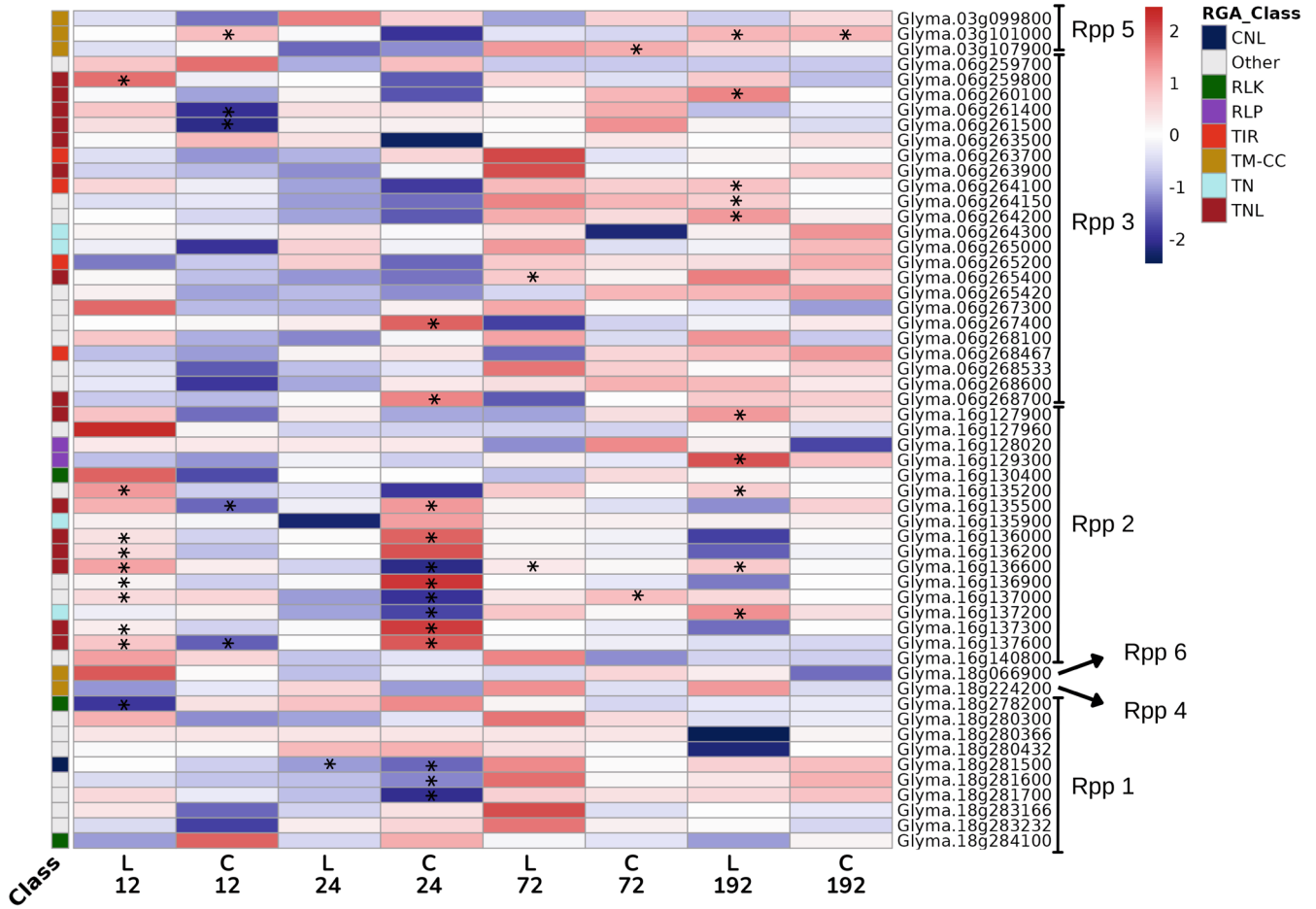

FIGURE 6 | Heatmap of RGAs expression at Rpp loci across all time points (12, 24, 72 and 192 HAI) and both water conditions (L: Water-limited/C: Control). The color scale indicates the $\log_2$ fold change for inoculated vs. not-inoculated plants, with red representing upregulation and blue representing downregulation. The RGA subclass of each gene is indicated by the color-coded bar on the left. Asterisks (*) denote DEGs. Annotations on the right indicate Rpp loci (Rpp1, Rpp2, Rpp3, Rpp4, Rpp5, and Rpp6) where these RGAs are located.

diminished as time passed and disease progressed. The number of differentially expressed genes showed a biphasic response, as seen before with the same pathosystem (van de Mortel et al. 2007), with defense-related genes being upregulated at earlier stages of infection (12 HAI), followed by a down-regulation (24 HAI) and then again being positively regulated at later time points (72 and 192 HAI).

We unveiled 33% more DEGs in plants with combined stress than in plants exposed to only the biotic stress. This higher number of DEGs reflects the broader range of plant responses necessary to maintain physiological homeostasis, coordinated by gene expression (Pandey et al. 2015; Zandalinas et al. 2018). Among the DEGs identified at 12 HAI, the strongest upregulated under water limitation were *Glyma.18g211100* (Peroxidase), *Glyma.18g267900* (Isoflavone 7-O-methyltransferase-like protein), *Glyma.02g007400* (Chitinase), and *Glyma.14g205200* (Cytochrome P450). Their expression levels were between 7 and 86 times higher in inoculated plants compared to non-inoculated plants under water limitation. The induction of these genes may lead to the production of phytoalexin, lignin, flavonoids, ABA, and chitin-pathogen digestion, which serve as chemical and physical barriers against fungal infection. These immune system components may also play roles in the response to water limitation (Almagro et al. 2009; Li et al. 2022; Zhang et al. 2017). Moreover, these genes are involved in other stress responses in soybean plants. Functional characterization of *Glyma.18g211100* has been shown to contribute to resistance against Cercospora leaf blight (Patel et al. 2024); *Glyma.18g267900* and *Glyma.02g007400* are associated with resistance to soybean cyst nematode (Hu et al. 2024; Zhang et al. 2017), while *Glyma.14g205200* was associated with drought resistance (Li et al. 2022). The plant's adaptability to diverse environmental conditions depends on a versatile defense network of genes with sometimes overlapping functions, which we also detected in our work.

The robust gene expression of plants exposed to combined stresses may stimulate transcriptional changes, leading to a faster and more intense response upon exposure to subsequent stress, as described for the priming effect (Mauch-Mani et al. 2017). Indeed, our data showed 25% more RGADE isoforms in plants exposed to combined stresses compared to only rust-inoculated plants. Additional evidence of the effects of combined stresses was indicated by the increased expression of RGAs in the early stages of infection, suggesting the activation of stress defense mechanisms under these conditions. Approximately 36% of the total RGADEs encoded receptor-like kinases (RLKs) and receptor-like proteins (RLPs). Considering that TM-LRR proteins constitute 30% of all RGAs in the genome,

our analysis revealed an enrichment of this receptor class under both experimental conditions—ASR inoculation with and without water limitation.

These proteins include pattern recognition receptors (PRRs), such as leucine-rich repeat receptor-like kinases (LRR-RLKs) and lectin receptor-like kinases (LecRLKs), which are known to recognize microbial-associated molecular patterns (MAMPs) and initiate pattern-triggered immunity (PTI) (Jones and Dangl 2006). In addition to their potential roles in pathogen recognition, some PRRs have also been associated with the perception of developmental and abiotic stress cues. Notably, water-limited plants showed a higher abundance of RLK-encoding RGADEs at 192 HAI, a time point corresponding to prolonged water deficit. These RLKs include genes predicted to belong to LRR-RLK and LecRLK subfamilies, which have been implicated in osmotic stress signaling and immune responses in other plant species (Osakabe et al. 2013). Based on these observations, we propose that water limitation may enhance the perception of multiple stress signals through overlapping receptor pathways, potentially leading, although insufficiently, to PTI response in susceptible plants. While this hypothesis remains to be explored experimentally, the transcription patterns observed help narrow down candidate RLKs for future functional validation, particularly those with stress-specific or time-dependent expression profiles. The apparent decline in defense-related gene expression at later stages suggests a shift toward effector-triggered susceptibility (ETS), a possibility that requires deeper investigation.

These observations raise the possibility that water limitation enhances the plant's perception of multiple stressors, potentially activating similar receptor types and leading to a stronger PTI response in susceptible plants. Despite the activation of these receptors, the overall diminished defense response observed in water-limited plants at later stages, when the fungus has already established itself and proliferated within the plant, suggests that effector-triggered susceptibility (ETS) significantly contributes to disease progression and severity, though this remains to be experimentally validated.

Throughout their infection stages, biotrophic fungi overcome plant defense systems by directing various effectors to impair plant defenses, whether suppressing PTI-activated responses after pathogen recognition or interacting with ETI receptors (Toruño et al. 2016). ASR fungus presents an efficient strategy to defeat responses upon that perception, leading to a strong down-regulation of genes related to plant defense at 24 HAI. The low representation of NBS-LRR-encoding genes among RGADEs at this time suggests a potential ETI response deactivation related to the expression and release of fungal effector proteins (Gupta et al. 2023). Other authors identified similar patterns for rusts, considering, for instance, time after inoculation for the analysis (Dobon et al. 2016; Pradeu et al. 2024). The reduced expression of defense genes in plants under water stress at 24 HAI is not as marked but still noticeable. Following this wave down, an increment toward positive net expression reaches its maximum at 192 HAI. With disease progress and fungal multiplication, the increase in MAMPs may result in a new wave of pathogen perception, reactivating the innate response at later moments. At that point, the induction of genes in which GO terms refer to plant defense, such as response to chitin and oxidative stress, has no effect since the disease has already been established and sporogenesis initiated.

The lower impact of the waves of recognition in water-limited plants, along with an increased expression of genes related to response to water deprivation, may indicate a redirection of efforts otherwise used for controlling the pathogen's development, resulting in a more robust plant susceptibility (Beattie 2011; Leisner et al. 2023).

We also analyzed the distribution of RGAs across soybean chromosomes and observed a tendency for these genes to accumulate near chromosomal ends, forming gene clusters. This is consistent with what has been described for RGAs in other crops' genomes, and is also similar to the distribution of protein-coding genes in the soybean genome (Christie et al. 2016; Liu et al. 2020; Rody et al. 2019; Wang et al. 2021). Notably, seven loci (Rpp1 to Rpp7) harboring combinations of RGAs conferring race-specific resistance to select *P. pachyrhizi* isolates have been genetically mapped in soybean (Childs et al. 2018). In our study, all loci except Rpp7 included differentially expressed RGAs (RGADEs), which accounted for 50% of all RGAs detected at Rpp loci, with 11 genes shared between water-limited and control conditions at specific time points. Among these, nine of these RGADEs were within the Rpp2 locus encoding disease resistance proteins of the TIR-NBS-LRR (TNLs) class. TNLs are active components of the ETI response, which seems suppressed in our experiments. Based on the earlier induction of Rpp2-associated genes in water-stressed plants, we speculate this locus plays a central role in *P. pachyrhizi* infection in the susceptible genotype studied. Functional validation will be needed to clarify the exact role of these loci. Still, pinpointing differentially expressed RGAs within important resistance regions offers a focused set of candidate genes that can be tested in future experiments to better understand their involvement in stress responses.

The Rpp2 locus offers additional insights into their coordinated expression and functional significance during pathogen attack. Among the RGAs, *Glyma.16g136000*, *Glyma.16g136900*, *Glyma.16g137000*, *Glyma.16g137300*, and *Glyma.16g137600* were all induced at 12 HAI under water-limited conditions. However, Glyma.16g136600 was consistently induced in water-limited plants but repressed 24 HAI in regularly watered plants, suggesting a role in abiotic stress. This may reflect an intricate network that ties the clustering of genes and possibly co-regulation to enable a rapid and localized immune response. The clustering of resistance genes is a common feature in plant genomes derived from selective pressures that favor the retention and duplication of genes involved in pathogen recognition and defense (Shao et al. 2016). However, despite the upregulation of these closely linked RGAs, particularly under water-limited conditions, the pathogen continues to establish and proliferate within the host.

We also identified DEGs related to abiotic stress that may contribute to compromising the coordination of responses under combined stress conditions. One example is the antagonistic interaction between abscisic acid (ABA) and salicylic acid (SA) signaling pathways. SA plays a central role in activating defense responses against biotrophic pathogens (Yasuda et al. 2008), while ABA is a key hormone regulating plant adaptation to

drought by controlling stomatal closure, osmotic balance, and other physiological processes. The crosstalk between ABA and SA has been shown to suppress the expression of pathogenesis-related genes, thereby impairing immune responses (Ghosh and Roychoudhury 2024). As a result, the activation of ABA pathways under drought stress may prioritize abiotic stress adaptation at the expense of biotic stress resistance, thereby facilitating pathogen establishment and proliferation, although hormonal levels were not directly assessed in the present study.

Exploring the regulatory networks governing RGA cluster modulation and their interactions with abiotic stress pathways is essential to better understanding the constraints on effective immunity in soybean genotypes. Our study emphasizes the significant modulation of soybean immune responses by water availability and identifies candidate genes for further investigation. These findings enhance our understanding of the complex interplay between abiotic and biotic stress responses, guiding the development of comprehensive strategies to manage drought and disease. Although no functional validation was conducted in this study, the identification of differentially expressed genes located in known resistance loci and enriched in defense-related processes supports their potential role in stress responses. These findings provide a valuable basis for future functional studies.

Acknowledgments

Dr. Quirijn de Jong van Lier (Soil Physics Laboratory, CENA/USP) for helping us to estimate the soil humidity at the permanent wilting point. Carlos Martinelli and GDM Seeds for their generous donations of soybean seeds. Dr. Sergio Pascholati and Ms. Sabrina Holz for sharing their *Phakopsora pachyrhizi* population. C.B.M.-V., L.A., and P.M. thank CNPq (The Brazilian National Council for Scientific and Technological Development) for research fellowships. G.H. was supported by Coordenação de Aperfeiçoamento de Pessoal de Nível Superior (CAPES 88887.671506/2022-00). This study was supported by the Fundação de Amparo à Pesquisa do Estado de São Paulo (FAPESP—2019/13191-5).

Conflicts of Interest

The authors declare no conflicts of interest.

Data Availability Statement

The data that support the findings of this study are openly available in NCBI Sequence Read Archive at https://www.ncbi.nlm.nih.gov/sra/PRJNA1137319, reference number PRJNA1137319. All scripts used in this study are available at the GitHub repository (https://github.com/GustavoHusein/soybean-RGA-combined-stress) and have been archived with a DOI via Zenodo: https://doi.org/10.5281/zenodo.15395777.

References

Alexa, A., and J. Rahnenfuhrer. 2024. "topGO: Enrichment Analysis for Gene Ontology. R Package Version 2.56.0." https://doi.org/10.1016/j.proenv.2011.05.005.

AliFakheri, B. 2014. "Marker-Assisted Selection for Disease Resistance: Applications in Breeding."

Almagro Armenteros, J. J., M. Salvatore, O. Emanuelsson, et al. 2019. "Detecting Sequence Signals in Targeting Peptides Using Deep Learning." *Life Science Alliance* 2: e201900429. https://doi.org/10.26508/lsa.201900429.

Almagro, L., L. V. Gómez Ros, S. Belchi-Navarro, R. Bru, A. Ros Barceló, and M. A. Pedreño. 2009. "Class III Peroxidases in Plant Defence Reactions." *Journal of Experimental Botany* 60: 377–390. https://doi.org/10.1093/jxb/ern277.

Alves, M. D. C., L. G. De Carvalho, E. A. Pozza, L. Sanches, and J. C. D. S. Maia. 2011. "Ecological Zoning of Soybean Rust, Coffee Rust and Banana Black Sigatoka Based on Brazilian Climate Changes." *Procedia Environmental Sciences* 6: 35–49. https://doi.org/10.1016/j.proenv.2011.05.005.

Barrs, H., and P. Weatherley. 1962. "A Re-Examination of the Relative Turgidity Technique for Estimating Water Deficits in Leaves." *Australian Journal of Biological Sciences* 15: 413–428.

Bateman, A., L. Coin, R. Durbin, et al. 2004. "The Pfam Protein Families Database." *Nucleic Acids Research* 32: D138–D141. https://doi.org/10.1093/nar/gkh121.

Beattie, G. A. 2011. "Water Relations in the Interaction of Foliar Bacterial Pathogens With Plants." *Annual Review of Phytopathology* 49: 533–555. https://doi.org/10.1146/annurev-phyto-073009-114436.

Boyer, J. S. 1995. "Biochemical and Biophysical Aspects of Water Deficits and the Predisposition to Disease." *Annual Review of Phytopathology* 33: 251–274. https://doi.org/10.1146/annurev.py.33.090195.001343.

Burdon, J. J., and J. Zhan. 2020. "Climate Change and Disease in Plant Communities." *PLoS Biology* 18: e3000949. https://doi.org/10.1371/journal.pbio.3000949.

Camejo, D., P. Rodríguez, M. A. Morales, J. M. Dell'Amico, A. Torrecillas, and J. J. Alarcón. 2005. "High Temperature Effects on Photosynthetic Activity of Two Tomato Cultivars With Different Heat Susceptibility." *Journal of Plant Physiology* 162: 281–289. https://doi.org/10.1016/j.jplph.2004.07.014.

Castro-Moretti, F. R., G. Husein, J. D. K. Nunes, et al. 2024. "Water Limitation Causes Early-Stage Metabolic Perturbation in the Interaction of Soybean and the Causal Agent of Asian Soybean Rust." https://doi.org/10.2139/ssrn.5042386.

Chang, J. H., Y.-S. Tai, A. J. Bernal, D. T. Lavelle, B. J. Staskawicz, and R. W. Michelmore. 2002. "Functional Analyses of the Pto Resistance Gene Family in Tomato and the Identification of a Minor Resistance Determinant in a Susceptible Haplotype." *Molecular Plant-Microbe Interactions* 15: 281–291. https://doi.org/10.1094/MPMI.2002.15.3.281.

Cheng, Y. T., L. Zhang, and S. Y. He. 2019. "Plant-Microbe Interactions Facing Environmental Challenge." *Cell Host & Microbe* 26: 183–192. https://doi.org/10.1016/j.chom.2019.07.009.

Childs, S. P., J. W. Buck, and Z. Li. 2018. "Breeding Soybeans With Resistance to Soybean Rust (*Phakopsora pachyrhizi*)." *Plant Breeding* 137: 250–261. https://doi.org/10.1111/pbr.12595.

Choudhary, A., and M. Senthil-Kumar. 2024. "Drought: A Context-Dependent Damper and Aggravator of Plant Diseases." *Plant, Cell & Environment* 47: 2109–2126. https://doi.org/10.1111/pce.14863.

Christie, N., P. A. Tobias, S. Naidoo, and C. Külheim. 2016. "The *Eucalyptus grandis* NBS-LRR Gene Family: Physical Clustering and Expression Hotspots." *Frontiers in Plant Science* 6: 1238. https://doi.org/10.3389/fpls.2015.01238.

Dean, R., J. A. L. Van Kan, Z. A. Pretorius, et al. 2012. "The Top 10 Fungal Pathogens in Molecular Plant Pathology." *Molecular Plant Pathology* 13: 804. https://doi.org/10.1111/j.1364-3703.2012.00822.x.

DeFalco, T. A., and C. Zipfel. 2021. "Molecular Mechanisms of Early Plant Pattern-Triggered Immune Signaling." *Molecular Cell* 81: 3449–3467. https://doi.org/10.1016/j.molcel.2021.07.029.

Delgado-Baquerizo, M., C. A. Guerra, C. Cano-Díaz, et al. 2020. "The Proportion of Soil-Borne Pathogens Increases With Warming at the

Global Scale." *Nature Climate Change* 10: 550–554. https://doi.org/10.1038/s41558-020-0759-3.

Dobon, A., D. C. E. Bunting, L. E. Cabrera-Quio, C. Uauy, and D. G. O. Saunders. 2016. "The Host-Pathogen Interaction Between Wheat and Yellow Rust Induces Temporally Coordinated Waves of Gene Expression." *BMC Genomics* 17: 380. https://doi.org/10.1186/s12864-016-2684-4.

Dodds, P. N., J. Chen, and M. A. Outram. 2024. "Pathogen Perception and Signaling in Plant Immunity." *Plant Cell* 36: 1465–1481. https://doi.org/10.1093/plcell/koae020.

Echeveste Da Rosa, C. R. 2015. "Asian Soybean Rust Resistance: An Overview." *Journal of Plant Pathology & Microbiology* 6: 307. https://doi.org/10.4172/2157-7471.1000307.

Engelbrecht, B. M. J., and T. A. Kursar. 2003. "Comparative Drought-Resistance of Seedlings of 28 Species of Co-Occurring Tropical Woody Plants." *Oecologia* 136: 383–393. https://doi.org/10.1007/s00442-003-1290-8.

Ferreira, M. F. 2010. "Caracterização Física do Solo." In *Física do Solo*, edited by Q. de Jong van Lier, 1–27. Sociedade Brasileira de Ciência do Solo.

Garcia, A., É. S. Calvo, R. A. Souza Kiihl, A. Harada, D. M. Hiromoto, and L. G. E. Vieira. 2008. "Molecular Mapping of Soybean Rust (*Phakopsora pachyrhizi*) Resistance Genes: Discovery of a Novel Locus and Alleles." *Theoretical and Applied Genetics* 117: 545–553. https://doi.org/10.1007/s00122-008-0798-z.

Gerós, H., M. M. Chaves, H. M. Gil, and S. Delrot. 2016. "A Molecular and Ecophysiological Perspective."

Ghini, R., E. Hamada, R. R. V. Gonçalves, L. Gasparotto, and J. C. R. Pereira. 2007. "Análise de Risco Das Mudanças Climáticas Globais Sobre a Sigatoka-Negra da Bananeira no Brasil." *Fitopatologia Brasileira* 32: 197–204. https://doi.org/10.1590/S0100-41582007000300003.

Ghosh, P., and A. Roychoudhury. 2024. "Molecular Basis of Salicylic Acid–Phytohormone Crosstalk in Regulating Stress Tolerance in Plants." *Brazilian Journal of Botany* 47: 735–750. https://doi.org/10.1007/s40415-024-00983-3.

Godoy, C. V., C. D. S. Seixas, R. M. Soares, F. C. Marcelino-Guimarães, M. C. Meyer, and L. M. Costamilan. 2016. "Asian Soybean Rust in Brazil: Past, Present, and Future." *Pesquisa Agropecuária Brasileira* 51: 407–421. https://doi.org/10.1590/S0100-204X2016000500002.

Goellner, K., M. Loehrer, C. Langenbach, U. Conrath, E. Koch, and U. Schaffrath. 2010. "*Phakopsora pachyrhizi*, the Causal Agent of Asian Soybean Rust." *Molecular Plant Pathology* 11: 169–177. https://doi.org/10.1111/j.1364-3703.2009.00589.x.

Gupta, Y. K., F. C. Marcelino-Guimarães, C. Lorrain, et al. 2023. "Major Proliferation of Transposable Elements Shaped the Genome of the Soybean Rust Pathogen *Phakopsora pachyrhizi*." *Nature Communications* 14: 1835. https://doi.org/10.1038/s41467-023-37551-4.

Hammond-Kosack, K. E., and J. D. G. Jones. 1997. "Plant Disease Resistance Genes." *Annual Review of Plant Biology* 48: 575–607. https://doi.org/10.1146/annurev.arplant.48.1.575.

Hu, H., L. Yi, D. Wu, et al. 2024. "Identification of Candidate Genes Associating With Soybean Cyst Nematode in Soybean (*Glycine max* L.) Using BSA-Seq." *PeerJ* 12: e18252. https://doi.org/10.7717/peerj.18252.

Hyten, D. L., G. L. Hartman, R. L. Nelson, et al. 2007. "Map Location of the Rpp1 Locus That Confers Resistance to Soybean Rust in Soybean." *Crop Science* 47: 837–838. https://doi.org/10.2135/cropsci2006.07.0484.

Hyten, D. L., J. R. Smith, R. D. Frederick, M. L. Tucker, Q. Song, and P. B. Cregan. 2009. "Bulked Segregant Analysis Using the GoldenGate Assay to Locate the Rpp3 Locus That Confers Resistance to Soybean Rust in Soybean." *Crop Science* 49: 265–271. https://doi.org/10.2135/cropsci2008.08.0511.

Ivancovich, A. J., G. Botta, M. Rivadaneira, E. Saieg, L. Erazzú, and E. Guillin. 2007. "First Report of Soybean Rust Caused by *Phakopsora pachyrhizi* on Phaseolus spp. in Argentina." *Plant Disease* 91: 111. https://doi.org/10.1094/PD-91-0111C.

Jones, J. D. G., and J. L. Dangl. 2006. "The Plant Immune System." *Nature* 444: 323–329. https://doi.org/10.1038/nature05286.

Jorge, V. R., M. R. Silva, E. A. Guillin, et al. 2015. "The Origin and Genetic Diversity of the Causal Agent of Asian Soybean Rust, *Phakopsora pachyrhizi*, in South America." *Plant Pathology* 64: 729–737. https://doi.org/10.1111/ppa.12300.

Kakumanu, A., M. M. R. Ambavaram, C. Klumas, et al. 2012. "Effects of Drought on Gene Expression in Maize Reproductive and Leaf Meristem Tissue Revealed by RNA-Seq1[W][OA]." *Plant Physiology* 160: 846–867. https://doi.org/10.1104/pp.112.200444.

Käll, L., A. Krogh, and E. L. L. Sonnhammer. 2004. "A Combined Transmembrane Topology and Signal Peptide Prediction Method." *Journal of Molecular Biology* 338: 1027–1036. https://doi.org/10.1016/j.jmb.2004.03.016.

Kelly, H. Y., N. S. Dufault, D. R. Walker, et al. 2015. "From Select Agent to an Established Pathogen: The Response to *Phakopsora pachyrhizi* (Soybean Rust) in North America." *Phytopathology* 105: 905–916. https://doi.org/10.1094/PHYTO-02-15-0054-FI.

Kim, D., B. Langmead, and S. L. Salzberg. 2015. "HISAT: A Fast Spliced Aligner With Low Memory Requirements." *Nature Methods* 12: 357–360. https://doi.org/10.1038/nmeth.3317.

King, Z. R., D. K. Harris, K. F. Pedley, et al. 2016. "A Novel *Phakopsora pachyrhizi* Resistance Allele (Rpp) Contributed by PI 567068A." *Theoretical and Applied Genetics* 129: 517–534. https://doi.org/10.1007/s00122-015-2645-3.

Konapala, G., A. K. Mishra, Y. Wada, and M. E. Mann. 2020. "Climate Change Will Affect Global Water Availability Through Compounding Changes in Seasonal Precipitation and Evaporation." *Nature Communications* 11: 3044. https://doi.org/10.1038/s41467-020-16757-w.

Krogh, A., B. Larsson, G. von Heijne, and E. L. L. Sonnhammer. 2001. "Predicting Transmembrane Protein Topology With a Hidden Markov Model: Application to Complete genomes11Edited by F. Cohen." *Journal of Molecular Biology* 305: 567–580. https://doi.org/10.1006/jmbi.2000.4315.

Langenbach, C., R. Campe, S. F. Beyer, A. N. Mueller, and U. Conrath. 2016. "Fighting Asian Soybean Rust." *Frontiers in Plant Science* 7: 797. https://doi.org/10.3389/fpls.2016.00797.

Le, D. T., R. Nishiyama, Y. Watanabe, et al. 2012. "Differential Gene Expression in Soybean Leaf Tissues at Late Developmental Stages Under Drought Stress Revealed by Genome-Wide Transcriptome Analysis." *PLoS One* 7: e49522. https://doi.org/10.1371/journal.pone.0049522.

Leisner, C. P., N. Potnis, and A. Sanz-Saez. 2023. "Crosstalk and Trade-Offs: Plant Responses to Climate Change-Associated Abiotic and Biotic Stresses." *Plant, Cell & Environment* 46: 2946–2963. https://doi.org/10.1111/pce.14532.

Leng, G., and J. Hall. 2019. "Crop Yield Sensitivity of Global Major Agricultural Countries to Droughts and the Projected Changes in the Future." *Science of the Total Environment* 654: 811–821. https://doi.org/10.1016/j.scitotenv.2018.10.434.

Li, M., H. Li, A. Sun, et al. 2022. "Transcriptome Analysis Reveals Key Drought-Stress-Responsive Genes in Soybean." *Frontiers in Genetics* 13: 1060529. https://doi.org/10.3389/fgene.2022.1060529.

Li, S., J. R. Smith, J. D. Ray, and R. D. Frederick. 2012. "Identification of a New Soybean Rust Resistance Gene in PI 567102B." *Theoretical and Applied Genetics* 125: 133–142. https://doi.org/10.1007/s00122-012-1821-y.

Liu, Y., H. Du, P. Li, et al. 2020. "Pan-Genome of Wild and Cultivated Soybeans." *Cell* 182: 162–176.e13. https://doi.org/10.1016/j.cell.2020.05.023.

Love, M. I., W. Huber, and S. Anders. 2014. "Moderated Estimation of Fold Change and Dispersion for RNA-Seq Data With DESeq2." *Genome Biology* 15: 550. https://doi.org/10.1186/s13059-014-0550-8.

Lupas, A., M. Van Dyke, and J. Stock. 1991. "Predicting Coiled Coils From Protein Sequences." *Science* 252: 1162–1164. https://doi.org/10.1126/science.252.5009.1162.

Mauch-Mani, B., I. Baccelli, E. Luna, and V. Flors. 2017. "Defense Priming: An Adaptive Part of Induced Resistance." *Annual Review of Plant Biology* 68: 485–512. https://doi.org/10.1146/annurev-arplant-042916-041132.

Michelmore, R. W., and B. C. Meyers. 1998. "Clusters of Resistance Genes in Plants Evolve by Divergent Selection and a Birth-And-Death Process." *Genome Research* 8: 1113–1130. https://doi.org/10.1101/gr.8.11.1113.

Mittler, R. 2006. "Abiotic Stress, the Field Environment and Stress Combination." *Trends in Plant Science* 11: 15–19. https://doi.org/10.1016/j.tplants.2005.11.002.

Osakabe, Y., K. Yamaguchi-Shinozaki, K. Shinozaki, and L.-S. P. Tran. 2013. "Sensing the Environment: Key Roles of Membrane-Localized Kinases in Plant Perception and Response to Abiotic Stress." *Journal of Experimental Botany* 64: 445–458. https://doi.org/10.1093/jxb/ers354.

Palliotti, A., O. Silvestroni, and D. Petoumenou. 2009. "Photosynthetic and Photoinhibition Behavior of Two Field-Grown Grapevine Cultivars Under Multiple Summer Stresses." *American Journal of Enology and Viticulture* 60: 189–198. https://doi.org/10.5344/ajev.2009.60.2.189.

Pandey, P., V. Ramegowda, and M. Senthil-Kumar. 2015. "Shared and Unique Responses of Plants to Multiple Individual Stresses and Stress Combinations: Physiological and Molecular Mechanisms." *Frontiers in Plant Science* 6: 723. https://doi.org/10.3389/fpls.2015.00723.

Paoletti, Danti, and Strati. 2001. "Pre- and Post-Inoculation Water Stress Affects *Sphaeropsis sapinea* Canker Length in *Pinus halepensis* Seedlings." *Forensic Pathology* 31: 209–218. https://doi.org/10.1046/j.1439-0329.2001.00237.x.

Patel, J., T. W. Allen, B. Buckley, et al. 2024. "Deciphering Genetic Factors Contributing to Enhanced Resistance Against Cercospora Leaf Blight in Soybean (*Glycine max* L.) Using GWAS Analysis." *Frontiers in Genetics* 15: 1377223. https://doi.org/10.3389/fgene.2024.1377223.

Pedley, K. F., A. K. Pandey, A. Ruck, L. M. Lincoln, S. A. Whitham, and M. A. Graham. 2019. "Rpp1 Encodes a ULP1-NBS-LRR Protein That Controls Immunity to *Phakopsora pachyrhizi* in Soybean." *Molecular Plant-Microbe Interactions* 32: 120–133. https://doi.org/10.1094/MPMI-07-18-0198-FI.

Perazzolli, M., G. Malacarne, A. Baldo, et al. 2014. "Characterization of Resistance Gene Analogues (RGAs) in Apple (Malus×Domestica Borkh.) and Their Evolutionary History of the Rosaceae Family." *PLoS One* 9: e83844. https://doi.org/10.1371/journal.pone.0083844.

Pertea, M., G. M. Pertea, C. M. Antonescu, T.-C. Chang, J. T. Mendell, and S. L. Salzberg. 2015. "StringTie Enables Improved Reconstruction of a Transcriptome From RNA-Seq Reads." *Nature Biotechnology* 33: 290–295. https://doi.org/10.1038/nbt.3122.

Pradeu, T., B. P. H. J. Thomma, S. E. Girardin, and B. Lemaitre. 2024. "The Conceptual Foundations of Innate Immunity: Taking Stock 30 Years Later." *Immunity* 57: 613–631. https://doi.org/10.1016/j.immuni.2024.03.007.

Ragazzi, A., S. Moricca, I. Dellavalle, and F. Mancini. 1995. "Infection of Cotton *Byfusarium oxysporum* f.sp.Vasinfectum as Affected by Water Stress." *Phytoparasitica* 23: 315–321. https://doi.org/10.1007/BF02981424.

Rahman, S. U., E. McCoy, G. Raza, Z. Ali, S. Mansoor, and I. Amin. 2023. "Improvement of Soybean; A Way Forward Transition From Genetic Engineering to New Plant Breeding Technologies." *Molecular Biotechnology* 65: 162–180. https://doi.org/10.1007/s12033-022-00456-6.

Rody, H. V. S., R. G. H. Bombardelli, S. Creste, L. E. A. Camargo, M.-A. Van Sluys, and C. B. Monteiro-Vitorello. 2019. "Genome Survey of Resistance Gene Analogs in Sugarcane: Genomic Features and Differential Expression of the Innate Immune System From a Smut-Resistant Genotype." *BMC Genomics* 20: 809. https://doi.org/10.1186/s12864-019-6207-y.

Schmutz, J., S. B. Cannon, J. Schlueter, et al. 2010. "Genome Sequence of the Palaeopolyploid Soybean." *Nature* 463: 178–183. https://doi.org/10.1038/nature08670.

Sekhwal, M. K., P. Li, I. Lam, X. Wang, S. Cloutier, and F. M. You. 2015. "Disease Resistance Gene Analogs (RGAs) in Plants." *International Journal of Molecular Sciences* 16: 19248. https://doi.org/10.3390/ijms160819248.

Shao, Z.-Q., J.-Y. Xue, P. Wu, et al. 2016. "Large-Scale Analyses of Angiosperm Nucleotide-Binding Site-Leucine-Rich Repeat Genes Reveal Three Anciently Diverged Classes With Distinct Evolutionary Patterns." *Plant Physiology* 170: 2095–2109. https://doi.org/10.1104/pp.15.01487.

Shen, W., S. Le, Y. Li, and F. Hu. 2016. "SeqKit: A Cross-Platform and Ultrafast Toolkit for FASTA/Q File Manipulation." *PLoS One* 11: e163962. https://doi.org/10.1371/journal.pone.0163962.

Silva, D. C. G., N. Yamanaka, R. L. Brogin, et al. 2008. "Molecular Mapping of Two Loci That Confer Resistance to Asian Rust in Soybean." *Theoretical and Applied Genetics* 117: 57–63. https://doi.org/10.1007/s00122-008-0752-0.

Singh, B. K., M. Delgado-Baquerizo, E. Egidi, et al. 2023. "Climate Change Impacts on Plant Pathogens, Food Security and Paths Forward." *Nature Reviews. Microbiology* 21: 640–656. https://doi.org/10.1038/s41579-023-00900-7.

Sunarti, S., C. Kissoudis, Y. Van Der Hoek, et al. 2022. "Drought Stress Interacts With Powdery Mildew Infection in Tomato." *Frontiers in Plant Science* 13: 845379. https://doi.org/10.3389/fpls.2022.845379.

Swett, C. L. 2020. "Managing Crop Diseases Under Water Scarcity." *Annual Review of Phytopathology* 58: 387–406. https://doi.org/10.1146/annurev-phyto-030320-041421.

Thornton, P. K., P. J. Ericksen, M. Herrero, and A. J. Challinor. 2014. "Climate Variability and Vulnerability to Climate Change: A Review." *Global Change Biology* 20: 3313–3328. https://doi.org/10.1111/gcb.12581.

Toruño, T. Y., I. Stergiopoulos, and G. Coaker. 2016. "Plant-Pathogen Effectors: Cellular Probes Interfering With Plant Defenses in Spatial and Temporal Manners." *Annual Review of Phytopathology* 54: 419–441. https://doi.org/10.1146/annurev-phyto-080615-100204.

Trivedi, P., B. D. Batista, K. E. Bazany, and B. K. Singh. 2022. "Plant-Microbiome Interactions Under a Changing World: Responses, Consequences and Perspectives." *New Phytologist* 234: 1951–1959. https://doi.org/10.1111/nph.18016.

van de Mortel, M., J. C. Recknor, M. A. Graham, et al. 2007. "Distinct Biphasic mRNA Changes in Response to Asian Soybean Rust Infection." *Molecular Plant-Microbe Interactions Journal* 20: 887–899. https://doi.org/10.1094/MPMI-20-8-0887.

van Niekerk, J. M., A. E. Strever, P. G. du Toit, F. Halleen, and P. H. Fourie. 2011. "Influence of Water Stress on Botryosphaeriaceae Disease Expression in Grapevines." *Phytopathologia Mediterranea* 50: S151–S165.

Velásquez, A. C., C. D. M. Castroverde, and S. Y. He. 2018. "Plant–Pathogen Warfare Under Changing Climate Conditions." *Current Biology* 28: R619–R634. https://doi.org/10.1016/j.cub.2018.03.054.

Vuong, T. D., D. R. Walker, B. T. Nguyen, et al. 2016. "Molecular Characterization of Resistance to Soybean Rust (*Phakopsora pachyrhizi* Syd. & Syd.) in Soybean Cultivar DT 2000 (PI 635999)." *PLoS One* 11: e0164493. https://doi.org/10.1371/journal.pone.0164493.

Wang, L., X. Yang, Y. Gao, and S. Yang. 2021. "Genome-Wide Identification and Characterization of TALE Superfamily Genes in Soybean (*Glycine max* L.)." *International Journal of Molecular Sciences* 22: 4117. https://doi.org/10.3390/ijms22084117.

Xue, Y., M. L. Warburton, M. Sawkins, et al. 2013. "Genome-Wide Association Analysis for Nine Agronomic Traits in Maize Under Well-Watered and Water-Stressed Conditions." *Theoretical and Applied Genetics* 126: 2587–2596. https://doi.org/10.1007/s00122-013-2158-x.

Yasuda, M., A. Ishikawa, Y. Jikumaru, et al. 2008. "Antagonistic Interaction Between Systemic Acquired Resistance and the Abscisic Acid–Mediated Abiotic Stress Response in Arabidopsis." *Plant Cell* 20: 1678–1692. https://doi.org/10.1105/tpc.107.054296.

Zandalinas, S. I., R. Mittler, D. Balfagón, V. Arbona, and A. Gómez-Cadenas. 2018. "Plant Adaptations to the Combination of Drought and High Temperatures." *Physiologia Plantarum* 162: 2–12. https://doi.org/10.1111/ppl.12540.

Zdobnov, E. M., and R. Apweiler. 2001. "InterProScan—An Integration Platform for the Signature-Recognition Methods in InterPro." *Bioinformatics* 17: 847–848. https://doi.org/10.1093/bioinformatics/17.9.847.

Zhang, H., S. Kjemtrup-Lovelace, C. Li, Y. Luo, L. P. Chen, and B.-H. Song. 2017. "Comparative RNA-Seq Analysis Uncovers a Complex Regulatory Network for Soybean Cyst Nematode Resistance in Wild Soybean (*Glycine soja*)." *Scientific Reports* 7: 9699. https://doi.org/10.1038/s41598-017-09945-0.

Supporting Information

Additional supporting information can be found online in the Supporting Information section. **Figure S1:** Top 15 most enriched biological process (BP) GO terms at each time point (12, 24, 72, and 192 HAI) in plants inoculated vs. non-inoculated under water limitation conditions. GO terms were ranked by *p*-value, and only the top 15 significant terms are shown for each time point. Graphs are displayed from top to bottom in chronological order. The enrichment score is plotted on the x-axis, and significance is indicated by the color gradient representing–log10 (*p*-value). **Figure S2:** Top 15 most enriched biological process (BP) GO terms at each time point (12, 24, 72, and 192 HAI) in plants inoculated vs. non-inoculated under normal water conditions. GO terms were ranked by *p*-value, and only the top 15 significant terms are shown for each time point. Graphs are displayed from top to bottom in chronological order. The enrichment score is plotted on the x-axis, and significance is indicated by the color gradient representing–log10 (*p*-value). **Figure S3:** Temporal distribution of RGADE expression under contrasting water conditions. The total number of RGADEs detected at each time point post-inoculation (12, 24, 72, and 192 HAI) is shown for plants under water limitation (blue line) and non-limiting water conditions (red line). **Figure S4:** Heatmap of expression profiles for all differentially expressed RGADEs across time points and water conditions. Expression values are represented as log2 fold changes (LFC) from pairwise comparisons of inoculated vs. non-inoculated plants. The heatmap includes eight experimental conditions: four infection time points (12, 24, 72, and 192 h after inoculation—HAI) under two water regimes (water-limited and non-limited). Columns represent each condition, and rows correspond to individual RGADEs. Genes are grouped by hierarchical clustering based on expression profiles, with RGA classes annotated by color on the left. **Table S1:** An overview of sequencing data quality statistics. **Table S2:** Significant differentially expressed genes for the Inoculated vs. Not Inoculated comparison for each time point and water condition. **Table S3:** Significant Biological Process enriched GO terms for all treatments and their associated statistics. **Table S4:** Statistical significance of the differences between the expression levels of control and water stressed plants for each plant defense related GO term and time point. **Table S5:** RGADE isoform expression per RGA class, water limitation condition and time point.